Photoionization-Efficiency Spectrum and Ionization Energy of the Cyanomethyl Radical CH_2CN and Products of the $N(^4S) + C_2H_3$ Reaction

R. Peyton Thorn Jr.,[†] Paul S. Monks,[‡] and Louis J. Stief*[,§]

Laboratory for Extraterrestrial Physics (Code 690), NASA/Goddard Space Flight Center, Greenbelt, Maryland 20071

Szu-Cherng Kuo,[||] Zhengyu Zhang,[⊥] Stuart K. Ross,[∇] and R. Bruce Klemm*[,#]

Brookhaven National Laboratory, Building 815, P.O. Box 5000, Upton, New York 11973-5000

Received: September 30, 1997; In Final Form: November 20, 1997

Photoionization efficiency (PIE) spectra of the CH_2CN radical were measured over the wavelength range λ = 115−130 nm using a discharge-flow−photoionization mass spectrometer coupled to a dispersed synchrotron-radiation source. The cyanomethyl radical was produced by the reaction $F + CH_3CN \rightarrow CH_2CN + HF$, and the PIE spectrum displayed steplike behavior near threshold. From the half-rise point of the initial step, a value of $10.28_0 \pm 0.01_0$ eV was obtained for the adiabatic ionization energy (IE) of CH_2CN based on five independent determinations. From a single measurement of the PIE spectrum and threshold for CD_2CN, we obtain IE(CD_2CN) = 10.24 eV. The experimental result for CH_2CN is compared with previous measurements, estimates, and calculations. The present PIMS study of the CH_2CN radical provides experimental measurements of the adiabatic ionization energy that are simultaneously the most direct and the most precise available. For the reaction $N(^4S) + C_2H_3$, the C_2H_2N radical product exhibits a PIE spectrum that may include CH_2CN along with another species that has a gradual threshold that is at a considerably longer wavelength than the steplike threshold of CH_2CN (derived from $F + CH_3CN$). A possible source of this difference is the contribution from higher-energy C_2H_2N isomers and/or from excited CH_2CN. In sharp contrast to the results for the $N(^4S) + C_2H_3$ reaction, no signal attributable to an isomer of the C_2D_2N radical was observed from the $N(^4S) + C_2D_3$ reaction. The C_2H_3N/C_2D_3N adducts from the $N(^4S) + C_2H_3/C_2D_3$ reactions were also studied. The adduct was observed to be solely CH_3CN for the $N(^4S) + C_2H_3$ reaction, while for $N(^4S) + C_2D_3$, the PIE spectrum appears to include significant contributions from both the lowest-energy isomer CD_3-CN and one or more higher-energy isomers.

Introduction

The cyanomethyl radical, CH_2CN, and the related molecule acetonitrile, CH_3CN, are prominent constituents in a wide variety of complex systems including hydrocarbon combustion,[1] thermal decomposition,[2] tropospheric and stratospheric chemistry of the earth's atmosphere,[3,4] and the chemistry of both interstellar clouds and the atmospheres of the outer planets.[5] It has recently been established that one or more isomers of the CH_2CN radical and the CH_3CN adduct molecule are primary products of the reaction of ground-state atomic nitrogen with the vinyl radical C_2H_3.[6]

The thermochemistry of CH_2CN and CH_3CN is complicated by the existence of several isomers for the C_2H_2N family of radicals and cations[7] and the C_2H_3N family of molecules and cations.[8−10] Of the six C_2H_2N radical isomers that could be expected as products of the $N + C_2H_3$ reaction, heats of formation of the neutral and ion are available for only three isomers.[7] For the five C_2H_3N molecule isomers potentially formed as adducts in this same reaction, heats of formation are known for all the neutral species and for four of the molecule ions.[8−10]

Present estimates of the ionization energy (IE) of the CH_2-CN radical are based on three distinct methods as reported in three very recent publications: the difference between experimentally determined values for $\Delta_fH°_{298}(CH_2CN^+)$ and $\Delta_fH°_{298}(CH_2CN)$;[7] a direct measurement[1] of IE(CH_2CN) via moderate-resolution electron-impact mass spectrometry (EIMS); a calculation[11] using more sophisticated methods and considerably larger basis sets than previously employed. Earlier estimates based on the first method are not reliable because of a problem with the value used for $\Delta_fH°_{298}(CH_2CN^+)$, which was based on the appearance energy of the radical ion formed by dissociative ionization of CH_3CN. Holmes and Mayer[7] have shown that, contrary to expectation, dissociative ionization of CH_3CN produces the lowest-energy cyclic isomer of the ion and not the linear CH_2CN^+ ion.

In this work we report the first direct determination of the CH_2CN photoionization efficiency (PIE) spectrum and photo-

† NAS/NRC Resident Research Associate. Email: ysrpt@lepvax.gsfc.nasa.gov.

‡ NAS/NRC Resident Research Associate. Present Address: Chemistry Department, University of Leicester, University Road, Leicester, LE1 7RH, England. Email: psm7@le.ac.uk.

§ Email: u1ljs@lepvax.gsfc.nasa.gov.

|| Present address: TRW Antenna Products Center, Mail Station 201/2055, Redondo Beach, CA 90278. Email: steven.kuo@trw.com.

⊥ Research Associate. Present address: Philips Lighting, Nanjing, Peoples Republic of China.

∇ Visiting Research Associate. Present address: Protection and Decontamination Department, CBD Porton Down, Salisbury, Wiltshire SP4 0JQ, U.K.

Email: klemm@sun2.bnl.gov.

* To whom correspondence should be sent.

S1089-5639(97)03164-2 CCC: $15.00
Published on Web 01/09/1998

ionization threshold. From the latter we obtain the first direct, high-resolution measurement of the ionization energy of the CH_2CN radical. Our result is compared with those from previous experimental and theoretical studies. We also report on the PIE spectra of the C_2H_2N radical and C_2H_3N adduct molecule formed in the reaction $N(^4S) + C_2H_3$. Products of the $N(^4S) + C_2D_3$ reaction are also investigated.

Experimental Section

Experiments were performed by employing a discharge-flow–photoionization mass spectrometer (DF–PIMS) apparatus coupled to beamline U11 at the National Synchrotron Light Source (NSLS) at Brookhaven National Laboratory. The apparatus and experimental procedures have been described in previous publications.[12–14]

The cyanomethyl radical was produced in a Teflon lined flow reactor by the reaction of atomic fluorine with an excess of acetonitrile:

$$F + CH_3CN \rightarrow CH_2CN + HF \qquad (1)$$

$$k_1(298\ K) = 1.2 \times 10^{-11}\ cm^3\ molecule^{-1}\ s^{-1}\ (ref\ 1)$$

Fluorine atoms were produced by passing a dilute mixture of F_2 (~5% in He) through a microwave discharge (<70 W, 2450 MHz). Typically, 90–100% of the F_2 was dissociated. The discharge region was at the upstream end of the flow tube and about 100 cm from the sampling nozzle. The CH_3CN/He mixture was introduced into the flow tube through the tip of the movable injector at a distance of 2.5 cm from the sampling nozzle. Under typical conditions the reaction was estimated to be 95% complete within 1.8 cm from the movable injector, assuming instantaneous mixing.

All experiments were conducted at ambient temperature ($T = 298 \pm 2$ K) and at a flow-reactor pressure of 4.1 ± 0.1 Torr with helium carrier gas. Flow velocities were approximately 1500 cm s^{-1}. We estimate $[CH_2CN]_0 \approx 1 \times 10^{13}$ molecules cm^{-3} as a maximum value in the $F + CH_3CN$ experiments.

For experiments on the products of the $N(^4S) + C_2H_3$ reaction, nitrogen atoms were produced in a microwave discharge of a dilute N_2/He mixture. Excited N and N_2 species from the discharge were quenched in a recombination volume[15] before the atomic N entered the back of the flow tube. Vinyl radicals were formed by the rapid reaction[16] of F atoms with an excess of C_2H_4, the F atoms being produced in a microwave discharge of F_2/He at the upstream end of the flow tube as described above. The C_2H_4/He mixture was introduced into the flow tube through a moveable injector, the tip of which was 10 cm from the sampling nozzle. At this distance the reaction time was about 7 ms, which ensured completion of the reaction sequence:

$$F + C_2H_4 \rightarrow HF + C_2H_3 \qquad (2a)$$

$$\rightarrow H + C_2H_3F \qquad (2b)$$

$$k_2(298\ K) = 2.7 \times 10^{-10}\ cm^3\ molecule^{-1}\ s^{-1}\ (ref\ 16)$$

$$N(^4S) + C_2H_3 \rightarrow products \qquad (3)$$

$$k_3(298\ K) = 7.7 \times 10^{-11}\ cm^3\ molecule^{-1}\ s^{-1}\ (ref\ 6)$$

By analogy with experiments on the $N(^4S) + C_2H_5$ reaction in this same flow system,[17] we estimate $[F]_0 \approx 3 \times 10^{13}$ molecules cm^{-3}, $[N]_0 \approx 3 \times 10^{13}$ molecules cm^{-3}, and $[C_2H_3]_0 \approx (5-10) \times 10^{12}$ molecules cm^{-3}.

The gaseous mixture in the flow reactor was sampled as a molecular beam into the sample chamber and subsequently into the photoionization source of the mass spectrometer. Ions were mass-selected with an axially aligned quadrupole mass filter, detected with a channeltron/pulse preamp, and then counted for preset integration times. Measurements of PIE spectra, the ratio of ion counts/light intensity versus wavelength, were made using tunable vacuum-ultraviolet (VUV) radiation at the NSLS. A monochromator with a normal-incidence grating (1200 lines/nm) was used to disperse the VUV light. For the CH_2CN radical product from $F + CH_3CN$ and for the C_2H_2N radical product from $N(^4S) + C_2H_3$, a LiF window ($\lambda > 105$ nm) was used to eliminate second- and higher-order radiation. For direct CH_3CN ionization and for the C_2H_3N adduct product from $N(^4S) + C_2H_3$, it was necessary to work below $\lambda = 105$ nm, and thus, the LiF window was not in place. In this case, corrections were made for second-order light by scanning the spectral range at one-half the wavelength range and one-half the wavelength step size. These short-wavelength scans were renormalized to reflect the intensity of second-order radiation on the first-order scan and subtracted from the raw data.[18] The intensity of the VUV light was monitored via a sodium salicylate coated window with an attached photomultiplier tube.

Acetonitrile (99%, Aldrich Chemical Co.), perdeuterated acetonitrile (99.8% D, Cambridge Isotope Laboratory), ethylene (research grade, 99.5%, MG Industries), and perdeuterated ethylene (98% D, Cambridge Isotope Laboratory) were all thoroughly outgassed by repeated freeze–pump–thaw cycles at $T = 77$ K. Helium (research grade, 99.9999%, MG Industries), nitrogen (99.999%, MG Industries), and fluorine (5% mixture of F_2 in helium, Cryogenic Rare Gases and MG Industries) were all used as supplied.

Results and Discussion

The PIE spectrum of the source molecule CH_3CN ($m/z = 41$) is shown in Figure 1A as an example of the PIMS experiment as well as a check on the wavelength calibration as determined by the zero-order setting,[12] which was adjusted at the beginning and checked at the end of each filling of the VUV ring. The ionization threshold, which is generally taken as the half-rise point of the first step (unless otherwise specified), is indicated in Figure 1B at $\lambda = 101.68$ nm. This corresponds to $IE(CH_3CN) = 12.19_4 \pm 0.01_3$ eV (where the uncertainty is conservatively estimated from the resolution), in excellent agreement with the recommended[9] value $12.19_4 \pm 0.00_5$ eV, which is also based on a photoionization study.[19] This level of agreement indicates that the wavelength calibration is reliable and that the threshold is not significantly perturbed by thermal effects.

The structure evident in the PIE spectrum of CH_3CN is a significant feature that is an unambiguous identifying characteristic or "fingerprint" of the molecule. This structure is related, according to Rider et al.,[19] to an autoionizing Rydberg state that converges to an excited state of the cation at 13.13 eV (~94.4 nm; see Figure 1A).

A. Ionization Energy of the CH_2CN Radical. The PIE spectrum for the CH_2CN radical ($m/z = 40$), produced in the reaction $F + CH_3CN$, is shown in Figure 2. This spectrum was obtained in the wavelength region $\lambda = 115.0-125.0$ nm at 0.20 nm intervals and a nominal resolution of 0.16 nm (fwhm). The somewhat restricted wavelength region is dictated by two

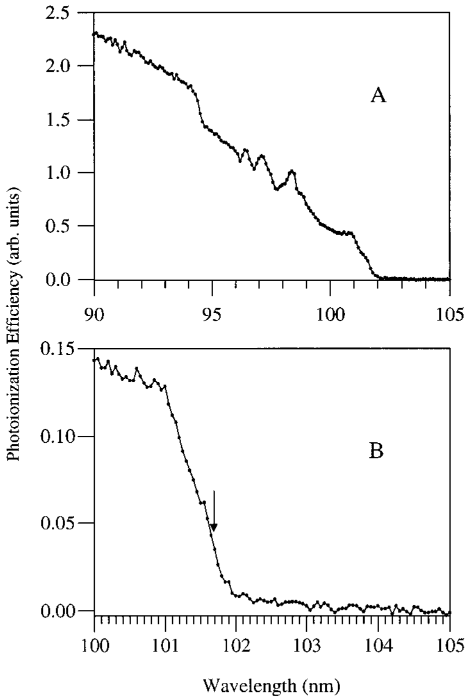

Figure 1. (A) Photoionization-efficiency spectrum of CH_3CN between $\lambda = 90.0$ and 105.0 nm at a nominal resolution of 0.16 nm with 0.1-nm steps. The photoionization efficiency is the ion counts at $m/z = 41$ divided by the light intensity in arbitrary units. $[CH_3CN] = 5.0 \times 10^{13}$ molecules cm^{-3}. The structure in this spectrum, with apparent peaks at about 98.4, 97.1, and 96.4 nm, is associated with a Rydberg series (see text) that converges to a limit at 94.45 nm. (B) Photoionization threshold region of CH_3CN between $\lambda = 100.0$ and 105.0 nm at a nominal resolution of 0.11 nm with 0.05-nm steps. The splitting in the threshold is presumably due to Jahn−Teller coupling in the CCN bending vibration.[19] The onset of ionization is at $\lambda = 101.68$ nm ($12.19_4 \pm 0.01_3$ eV).

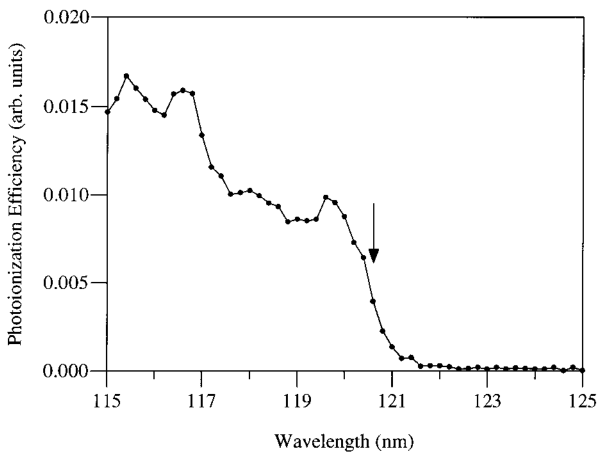

Figure 2. Photoionization-efficiency spectrum and threshold of CH_2-CN between $\lambda = 115.0$ and 125.0 nm. The onset of ionization is at $\lambda = 120.6$ nm ($10.28_1 \pm 0.01_4$ eV). $[CH_3CN]_0 = 2.1 \times 10^{14}$ molecules cm^{-3} and $[F_2]_0 = 8.5 \times 10^{12}$ molecules cm^{-3}.

factors. The first is our preference to avoid, when possible, operating without the LiF window and therefore to avoid the need to correct for second-order light from the monochromator. This limits the shorter-wavelength limit to above the LiF cutoff, i.e., above the minimum $\lambda = 105$ nm where the UV flux is greatly reduced even for a clean window not damaged via F-center formation. The second factor is the location of the photoionization threshold, which determines the longer-wavelength limit to be scanned.

There is only limited structure discernible in Figure 2, which may be due to either autoionizing Rydberg states and/or cation vibrational levels above $n = 0$. From Figure 2 a threshold wavelength of $\lambda = 120.6$ nm is obtained corresponding to IE-(CH_2CN) = 10.28_1 eV. The results of five independent determinations of IE(CH_2CN) that covered various wavelength ranges with wavelength step intervals of 0.1 or 0.2 nm and nominal resolutions of 0.1_3−0.1_6 nm yield a simple average of $10.28_0 \pm 0.01_0$ eV for IE(CH_2CN) where the precision is at the 2σ level. From a single measure of the PIE spectrum and threshold for CD_2CN (formed via the F + CD_3CN reaction), we obtain a threshold wavelength of $\lambda = 121.1$ nm. This wavelength corresponds to IE(CD_2CN) = 10.24 eV, which is 0.04 eV lower than the value for CH_2CN. The CD_2CN PIE spectrum is essentially the same as that for CH_2CN shown in Figure 2.

It must be emphasized that the rather sharp transition observed at the onset of ionization (Figure 2) for the CH_2CN radical and the fact that the lowest state of the cation is the cyclic isomer[7] mean that we are observing the transition to the linear CH_2-CN^+ structure and not the transition to the lower-energy cyclic cation. The latter transition would have very low probability (vanishingly small Franck−Condon factors) due to the large change in geometry.

A comparison of our result for IE(CH_2CN) with previous estimates is presented in Table 1. These estimates include an earlier measurement[20] via EIMS as well as a very recent one[1] using the same technique. Upper and lower limits are available from PIMS studies that employed rare-gas resonance lamps;[21,22] it was observed that CH_2CN was readily detected and monitored with an Ar lamp/LiF window (11.6, 11.8 eV)[21,22] but not with a Kr lamp/MgF_2 window (10.0, 10.6 eV).[22] A value for IE(CH_2-CN) may also be determined from the difference between the recently measured values for $\Delta_f H$(CH_2CN^+) and $\Delta_f H$(CH_2-CN).[7,9] Finally, there is a very recent theoretical calculation that employed very large basis sets.[11] It may be seen in Table 1 that our value of IE(CH_2CN) = 10.28_0 eV agrees best with the two previous estimates that should be the more accurate and reliable: 10.1 eV determined from the difference in the heats of formation of the cation and neutral[7] and 10.20 eV calculated theoretically.[11] The energy resolution in the two direct EIMS studies[1,20] of the CH_2CN free radical was at least an order of magnitude less than that in our PIMS study. The recent value[1] (10.5 ± 0.3 eV) agrees with our more precise result within their stated uncertainty, while the older value[20] (10.87 ± 0.10 eV) is too large by an amount that far exceeds the combined experimental uncertainties. This could be due to a significant error in the older measurements and/or a substantial underestimation of the experimental uncertainty. The resonance-lamp PIMS studies do give satisfactory upper and lower limits to our result if it is recognized that the more energetic Kr resonance line at $\lambda = 116.5$ nm (10.6 eV) is much weaker in a typical Kr resonance lamp (20% of the 10.0 eV line at $\lambda = 123.6$ nm) and may be further attenuated by deposits on the MgF_2 window. Thus, a better lower limit is probably IE(CH_2-CN) > 10.0 eV. A value for IE(CH_2CN) cannot be obtained from the appearance energy of the $C_2H_2N^+$ fragment ion from CH_3CN because the fragment ion formed is the ground-state cyclic isomer.[7] In summary, the present PIMS study of the CH_2-CN radical provides an experimental measurement of the adiabatic ionization energy of this species that is simultaneously the most direct and the most precise available.

B. Free-Radical Products at *m/z* = 40 and 42 of the N(^{4}S) + C_2H_3/C_2D_3 Reactions. At a photon energy of 11.3 eV (λ =

TABLE 1: Comparison of Values for IE(CH_2CN)

IE(CH_2CN) (eV)	method[a]	ref
10.87 ± 0.10	EIMS	Pottie and Lossing (1961)[20]
$<11.6-11.8$	PIMS/Ar lamp	Park and Gutman (1983)[21]
10.0	derived	Lias et al. (1993)[9]
$>10.0-10.6$	PIMS/Kr lamp	Masaki et al. (1995)[22]
10.1 ± 0.2^b	$\Delta_f H(CH_2CN^+) - \Delta_f H(CH_2CN)$	Holmes and Mayer (1995)[7]
10.5 ± 0.3	EIMS	Hoyermann and Seeba (1995)[1]
10.20 ± 0.05	ab initio calculation	Horn et al. (1995)[11]
$10.28_0 \pm 0.01_0$	PIMS/synchrotron	this study

[a] EIMS, electron impact mass spectrometry; PIMS, photoionization mass spectrometry. [b] This value was derived from heats of formation of the CH_2CN radical and the cation at $T = 298$ K and strictly should not be equated to the IE. However, the error in doing so is only the difference in the integrated heat capacities of CH_2CN^+ and CH_2CN, which is probably about 1−2 kJ mol^{-1} (0.01−0.02 eV).

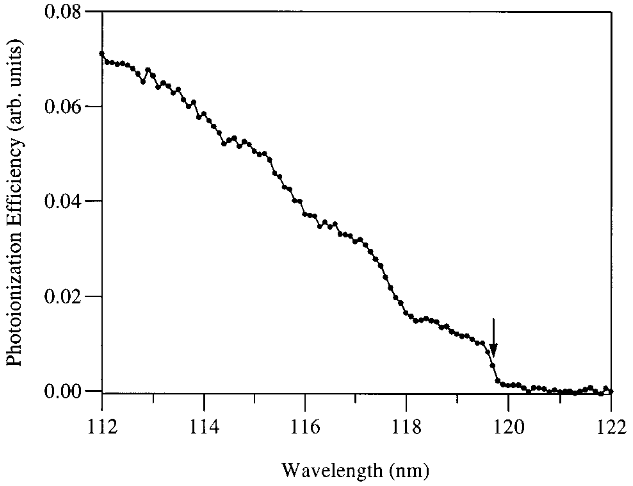

Figure 3. Photoionization-efficiency spectrum of C_2H_3F between $\lambda = 112.0$ and 122.0 nm at a nominal resolution of 0.13 nm with 0.1-nm steps. The onset of ionization is at $\lambda = 119.7$ nm ($10.35_8 \pm 0.01_1$ eV). $[C_2H_4]_0 = 7.7 \times 10^{14}$ molecules cm^{-3} and $[F_2]_0 = 2.8 \times 10^{13}$ molecules cm^{-3}.

110 nm) in the $N(^4S) + C_2H_3$ system, major peaks at $m/z = 40$ and $m/z = 46$ are observed. The feature at $m/z = 46$ is present in the absence of N and is due to C_2H_3F formed along with C_2H_3 in the reaction of F with C_2H_4[16] (see reaction 2). The PIE spectrum of C_2H_3F formed in reaction 2b is shown in Figure 3. The photoionization threshold is at $\lambda = 119.7$ nm. This corresponds to IE(C_2H_3F) = 10.35_8 eV, which agrees well with the recommended[9] value of 10.36_3 eV and again demonstrates that the wavelength calibration is reliable. We also note the absence of significant signal above background due to "hot bands", which indicates that any excess internal energy ($\Delta_r H°_{298} = -52.7$ kJ mol^{-1})[9] is rapidly lost via collisions in the flow tube.

The PIE spectrum of the C_2H_2N radical ($m/z = 40$) produced in the reaction $N(^4S) + C_2H_3$ is shown in Figure 4 (curves "b" and "c"),

$$N(^4S) + C_2H_3 \rightarrow C_2H_2N + H \tag{3a}$$

This spectrum was obtained in the wavelength region $\lambda = 115.0-130.0$ nm at 0.2-nm intervals with a nominal resolution of 0.17 nm. The spectrum (Figure 4, curves "b" and "c") differs in two significant ways from that of the CH_2CN radical isomer formed via $F + CH_3CN$ and recorded under similar experimental conditions (Figure 4, curve "a"). First, although the CH_2CN spectrum shows a sharp, steplike transition at threshold, the C_2H_2N isomer (or isomers) formed via $N(^4S) + C_2H_3$ displays a gradually decreasing signal as wavelength increases. Second, although the threshold for the radical product of $N(^4S) + C_2H_3$

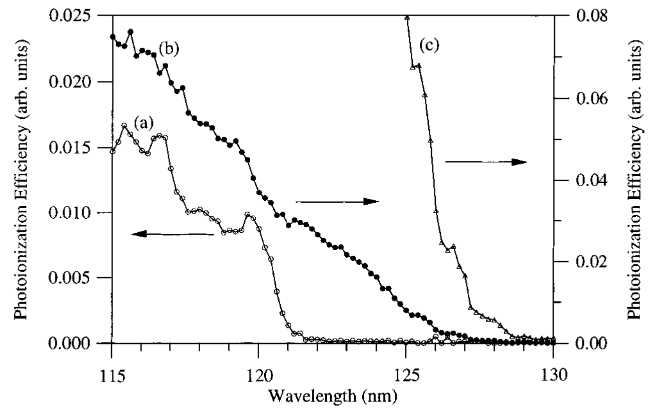

Figure 4. (a) Curve (○) is the photoionization-efficiency spectrum of CH_2CN radical from Figure 2. (b) Curve (●) is the photoionization-efficiency spectrum of C_2H_2N radical (formed in the $N(^4S) + C_2H_3$ reaction) between $\lambda = 115.0$ and 130.0 nm. $[C_2H_4]_0 = 5.3 \times 10^{14}$ molecules cm^{-3}, $[F_2]_0 = 2.7 \times 10^{13}$ molecules cm^{-3}, and $[N_2]_0 = 1.9 \times 10^{15}$ molecules cm^{-3}. (c) Curve (△) is the same as curve in (b) expanded by a factor of 10 to highlight the threshold region.

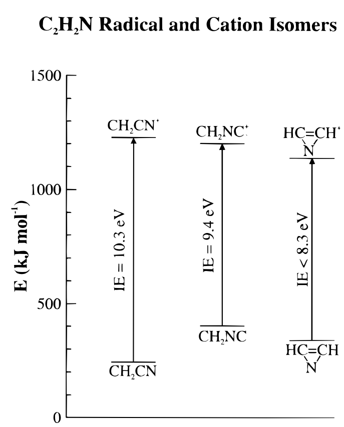

Figure 5. Enthalpies of formation and ionization energies of CH_2CN, CH_2NC, and cyclic C_2H_2N (see text for details and references).

is difficult to define, it is at a considerably longer wavelength ($\lambda > 128.6$ nm, IE < 9.64 eV) than the sharp threshold observed for the CH_2CN isomer ($\lambda = 120.6$ nm, IE = 10.28_0 eV). The obvious conclusion is that the C_2H_2N radical product from the $N(^4S) + C_2H_3$ reaction may not be solely identified with the equilibrated linear ground-state isomer CH_2CN. The enthalpies of formation[7,9] and IEs[1,7,11] of CH_2CN, CH_2NC, and cyclic C_2H_2N are summarized in Figure 5. Although the IEs for the CH_2NC isomer (IE = 9.4 eV, $\lambda = 132$ nm)[7] and the cyclic isomer

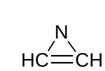

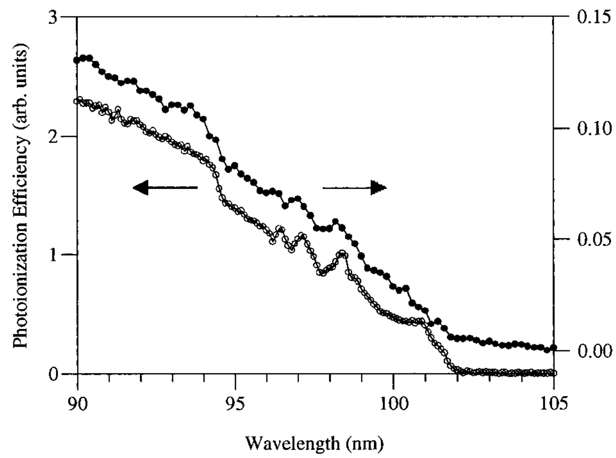

Figure 6. Upper curve (●) is the photoionization-efficiency spectrum of CH_3CN formed in the $N(^4S) + C_2H_3$ reaction between $\lambda = 90.0$ and 105.0 nm. $[C_2H_4]_0 = 4.1 \times 10^{14}$ molecules cm^{-3}, $[F_2]_0 = 3.5 \times 10^{13}$ molecules cm^{-3}, and $[N_2]_0 = 1.1 \times 10^{15}$ molecules cm^{-3}. Lower curve (○) is the photoionization-efficiency spectrum of CH_3CN from Figure 1A.

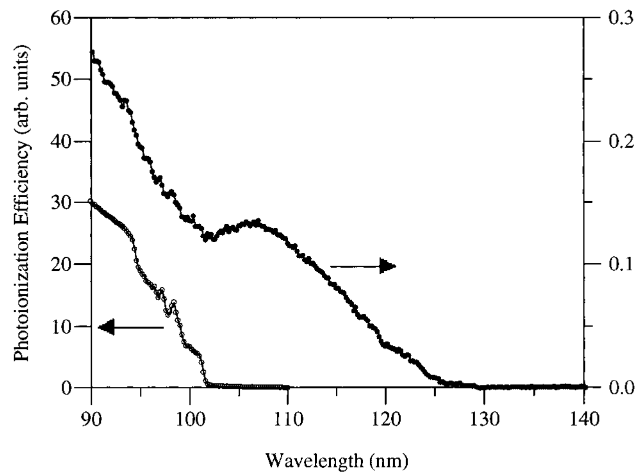

Figure 7. Upper curve (●) is the photoionization-efficiency spectrum of C_2D_3N formed in the $N(^4S) + C_2D_3$ reaction between $\lambda = 90.0$ and 140.0 nm. $[C_2D_4]_0 = 3.7 \times 10^{14}$ molecules cm^{-3}, $[F_2]_0 = 3.5 \times 10^{13}$ molecules cm^{-3}, and $[N_2]_0 = 1.1 \times 10^{15}$ molecules cm^{-3}. Lower curve (○) is the photoionization-efficiency spectrum of CD_3CN between $\lambda = 90.0$ and 110.0 nm at the same resolution and step size as those for the upper trace. $[CD_3CN]_0 = 1.1 \times 10^{14}$ molecules cm^{-3}.

(IE < 8.3 eV, λ > 149 nm)[7] do not appear to match that for the species detected in this work, there are no reported PIE spectra for these isomers, and therefore, their photoionization threshold behavior is unknown. The IEs of the three other C_2H_2N isomers,

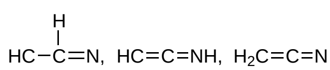

are unknown as are their heats of formation. Thus, the potential contribution of these isomers to the C_2H_2N product spectrum in curves b and c of Figure 4 cannot be evaluated at present. A contribution from thermally excited CH_2CN, which would extend the threshold to lower energies as observed, cannot be ruled out. However, our experience has been that rapid thermalization of reaction products is generally achieved in the flow reactor. For example, in the present study there is no compelling evidence for thermal excitation in the PIE spectra of either the C_2H_3F product (Figure 3) or the CH_3CN product (Figure 6), both of which are formed initially "hot". We are therefore unable to identify the C_2H_2N product at this time. Further studies on both the C_2H_2N radical product of the $N(^4S) + C_2H_3$ reaction and on the thermochemical properties of all the C_2H_2N radical isomers are clearly required.

A search for the PIE signal of the expected C_2D_2N radical ($m/z = 42$) from the reaction $N(^4S) + C_2D_3$ proved to be entirely negative. Under conditions very similar to these employed above for detection of C_2H_2N from $N(^4S) + C_2H_3$, no net signal above background was detected. This indicates a yield of less than 1% for C_2D_2N compared to a yield of 80% (ref 6) for C_2H_2N. We have no explanation at this time for such a strong and unexpected isotope effect.

C. Adduct Molecule Products at $m/z = 41$ and 44 of the $N(^4S) + C_2H_3/C_2D_3$ Reactions. The PIE spectrum of the C_2H_3N adduct molecule ($m/z = 41$) formed in the $N(^4S) + C_2H_3$ reaction is shown in Figure 6 (upper curve). This spectrum was measured over the wavelength region $\lambda = 90.0-105.0$ nm at 0.2-nm intervals with a nominal resolution of 0.1_0 nm. The ionization threshold is at $\lambda = 101.6$ nm (12.20 eV). This result is in excellent agreement with the PIE threshold for CH_3CN shown in the lower curve in Figure 6 ($\lambda = 101.68$ nm, IE $= 12.19_4$ eV) and the recommended[9] value of IE(CH_3CN) $= 12.19_4$ eV. Additionally, the structure in the PIE spectrum of the C_2H_3N adduct closely matches that of acetonitrile. The IEs of three of the remaining C_2H_3N isomers are known to be considerably lower than our observed value of 12.20 eV, i.e., 11.2 eV for CH_3NC,[9] about 10.1 eV for the cyclic isomer 2*H*-azarine[8,9]

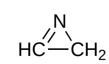

and ~8.3 eV for $H_2C{=}C{=}NH$ (ketene imine).[6,9,10] The IE is unknown for the isomer vinyl nitrene

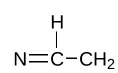

We therefore conclude that the lowest-energy isomer, CH_3CN, is the major and probably exclusive C_2H_3N adduct isomer ($m/z = 41$) formed in the $N(^4S) + C_2H_3$ reaction under the experimental conditions of the present photoionization study and the previous electron-impact study.[6]

The identity of the adduct molecule is much less clear for the $N(^4S) + C_2D_3$ reaction. The PIE spectrum of the C_2D_3N adduct molecule ($m/z = 44$) is shown in the upper curve of Figure 7. The spectrum was obtained in the wavelength region 90.0−140.0 nm at 0.2-nm intervals and a nominal resolution of 0.1_0 nm. The difference between this spectrum and that obtained for deuterated acetonitrile (CD_3CN) under the same conditions (Figure 7, lower curve) is immediately obvious and striking. In the region $\lambda = 90-100$ nm, both spectra exhibit the same fingerprint structure and a generally decreasing signal with increasing wavelength. But at wavelengths larger than 100 nm, the authentic CD_3CN signal continues to decrease with a well-defined step threshold at $\lambda = 101.4$ nm. In contrast, the C_2D_3N spectra from the $N(^4S) + C_2D_3$ reaction exhibits a signal increase above $\lambda = 100$ nm, reaching a maximum near $\lambda = 106$ nm and then decreasing rather continuously and gradually to a threshold at approximately $\lambda = 129.2$ nm (9.59_6 eV). In the C_2D_3N spectrum (Figure 7, upper curve) the structure in the region $\lambda = 90-100$ nm due to CD_3CN and the unidentified structure in the region $\lambda = 100-125$ nm was confirmed by replicate runs. The 9.59_6-eV threshold does not correspond to the IE of the nondeuterated versions of the isomers

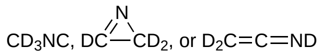

but only the ketene imine isomer may be excluded from contribution. We therefore conclude that the C_2D_3N adduct formed in the reaction $N(^4S) + C_2D_3$ includes a significant contribution from the lowest-energy isomer CD_3CN (acetonitrile), as well as possible contributions from

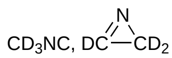

and perhaps

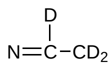

(vinyl nitrene) or other unidentified isomers. A more definitive conclusion must await information on the IEs of such isomers.

The difference in the adduct isomers observed for the $N(^4S) + C_2H_3$ and $N(^4S) + C_2D_3$ reactions may be related to the fate of the initially formed adduct, which is very likely 2*H*-azarine if N adds across the C═C double bond (to form the cyclic isomer) or else vinyl nitrene if N attacks the C atom having only one H attached (to form the biradical). Subsequent isomerization of either of these isomers to the lowest-energy CH_3CN isomer involves an H-atom transfer to the adjacent carbon.[10] For the present reaction conditions (∼7-ms reaction time), this process is facile for the protonated species but inhibited for the deuterated species. This behavior is consistent with a mechanism that involves a 1,2-H/D shift, the kinetics of which are controlled by tunneling.

Notes Added in Proof. After the present paper was accepted for publication, a photoelectron spectroscopy (PES) study was published (Shea, D. A.; Steenvoorden, J. J. M.; Chen, P. *J. Phys. Chem. A* **1997**, *101*, 9728) that reports a value of 10.30 ± 0.04 eV for the adiabatic ionization energy of CH_2CN radical. In that study, CH_2CN was generated via the thermal dissociation of "chloro-, bromo-, or iodoacetonitrile ... at temperatures >1200 K (10-ms contact time)". Since the PES study employed both a different measurement technique and a different radical-generation procedure, we believe that the good agreement between our two studies demonstrates the definitive determination of $IE(CH_2CN)$.

Acknowledgment. The work at BNL was supported by the Chemical Sciences Division, Office of Basic Energy Sciences, U.S. Department of Energy (under Contract No. DE-AC02-786CH00016) and the Laboratory Directed Research and Development Program at Brookhaven National Laboratory. The work at GSFC was supported by the NASA Planetary Atmospheres Research Program and the NASA Upper Atmosphere Research Program. R.P.T. and P.S.M. thank the NAS/NRC for the award of a research associateship.

References and Notes

(1) Hoyermann, K.; Seeba, J. *Z. Phys. Chem.* **1995**, *188*, 215.

(2) Lifshitz, A.; Moran, A.; Bidasic, S. *Int. J. Chem. Kinet.* **1987**, *19*, 61.

(3) Kurylo, M. J.; Knable, G. L. *J. Phys. Chem.* **1984**, *88*, 3305.

(4) Poulet, G.; Laverdet, J. L.; Jourdain, J. L.; LeBras, G. *J. Phys. Chem.* **1984**, *88*, 6259.

(5) (a) Irvine, W. M.; Friberg, P.; Hjalmarson, A.; Ishikawa, S.; Kaifu, N.; Kawaguchi, K.; Madden, S. C.; Matthews, H. E.; Ohishi, M.; Saito, S.; Suzuki, H.; Thaddeus, P.; Turner, B. E.; Yamamoto, S.; Ziurys, L. M. *Astrophys. J.* **1988**, *334*, L107. (b) Solomon, P. M.; Jefferts, K. B.; Penzlas, A. A.; Wilson, R. W. *Astrophys. J.* **1971**, *168*, L107. (c) Bezard, B.; Marten, A.; Paubert, G. *Bull. Am. Astron. Soc.* **1993**, *25*, 1100.

(6) Payne, W. A.; Monks, P. S.; Nesbitt, F. L.; Stief, L. J. *J. Chem. Phys.* **1996**, *104*, 9808.

(7) Holmes, J. L.; Mayer, P. M. *J. Phys. Chem.* **1995**, *99*, 1366.

(8) Bock, H.; Dammel, R. *Chem. Ber.* **1987**, *120*, 1971. Note that the value of 10.58 eV listed in this paper is for the vertical transition, whereas the value given here and in ref 9 is an estimate of the threshold value (i.e., a value that may approximate the adiabatic transition).

(9) Lias, S. G.; Liebman, J. F.; Levin, R. D.; Kafafi, S. A. *Positive Ion Energetics*, Version 2.0; NIST Standard Reference Database 19A; NIST: Gaithersburg, MD, 1993.

(10) Doughty, A.; Bacskay, G. B.; Mackie, J. C. *J. Phys. Chem.* **1994**, *98*, 13546.

(11) Horn, M.; Oswald, M.; Oswald, R.; Botschwina, P. *Ber. Bunsen-Ges. Phys. Chem* **1995**, *99*, 323.

(12) Kuo, S.-C.; Zhang, Z.; Klemm, R. B.; Liebman, J. F.; Stief, L. J.; Nesbitt, F. L. *J. Phys. Chem.* **1994**, *98*, 4026.

(13) Monks, P. S.; Stief, L. J.; Krauss, M.; Kuo, S. C.; Zhang, Z.; Klemm, R. B. *J. Phys. Chem.* **1994**, *98*, 10017.

(14) Buckley, T. J.; Johnson, R. D., III.; Huie, R. E.; Zhang, Z.; Kuo, S.-C.; Klemm, R. B. *J. Phys. Chem.* **1995**, *99*, 4879.

(15) Stief, L. J.; Marston, G.; Nava, D. F.; Payne, W. A.; Nesbitt, F. L. *Chem. Phys. Lett.* **1988**, *147*, 570.

(16) (a) Nesbitt, F. L.; Monks, P. S.; Scanlon, M.; Stief, L. J. *J. Phys. Chem.* **1994**, *98*, 4307 and references therin. (b) Slagle, I. R.; Gutman, D. *J. Phys. Chem.* **1983**, *87*, 1818.

(17) Stief, L. J.; Nesbitt, F. L.; Payne, W. A.; Kuo, S. C.; Tao, W.; Klemm, R. B. *J. Chem. Phys.* **1995**, *102*, 5309.

(18) Grover, J. R.; Walters, E. A.; Newman, J. K.; White, M. C. *J. Am. Chem. Soc.* **1985**, *107*, 7329 and references therein.

(19) Rider, D. M.; Ray, G. W.; Darland, E. J.; Leroi, G. E. *J. Chem. Phys.* **1981**, *74*, 1652.

(20) Pottie, R. F.; Lossing, F. P. *J. Am. Chem. Soc.* **1961**, *83*, 4737.

(21) Park, J.-Y.; Gutman, D. *J. Phys. Chem.* **1983**, *87*, 1844.

(22) Masaki, A.; Tsunashima, S.; Washida, N. *J. Phys. Chem.* **1995**, *99*, 13126.